Methodology for Determining the Die-Off Coefficient of Enterococci in the Conditions of Transport through the Karst Aquifer—Case Study: Bokanjac–Poličnik Catchment

Željko Šreng [1],[*] , Goran Lončar [2] and Marin Grubišić [1]

[1] University of Osijek, Faculty of Civil Engineering and Architecture Osijek, 3 Vladimir Prelog Street, HR–31 000 Osijek, Croatia; marin.grubisic@gfos.hr

[2] University of Zagreb, Faculty of Civil Engineering, 26 Fra Andrija Kačić-Miošić Street, HR–10 000 Zagreb, Croatia; gloncar@grad.hr

[*] Correspondence: zsreng@gfos.hr; Tel.: +385-95-529-1398

Abstract: This paper presents the methodology for determining the die-off coefficient of faecal indicator bacteria (enterococci) when transported in a karst environment. The main problem in exploring karst environments, which this methodology strives to cope with, is lack of field measurements, poor data on karst rock formation, fractures and channels within it, and groundwater level dynamics. The analysed karst catchment (Bokanjac–Poličnik) is situated in the hinterland of the city of Zadar (Republic of Croatia) and covers an area of 235.07 km^2. In the water supply wells within the analysed catchment, a frequent occurrence of enterococci was observed. The proposed methodology consists of two basic steps. Preliminary analyses as the initial step were used in the accumulation of certain assumptions related to the detection of increased concentrations of enterococci as well as in determination of the potential source of pollution. In the second step, the analytical model was constructed with the aim of resolving processes of sorption and die-off and determining the dominant factor in the process of natural removal of enterococci when transported in karst environment. Within the model, two parts of the pollutant transport are integrated: vertical percolation and horizontal seepage flow and transport. The mean value of the total die-off coefficient by transport through the unsaturated zone in the analysed case is $k_{tot} = 8.25$. Within the saturated zone the total die-off coefficient k_{tot} is within the limits of 0.1 and 0.5.

Keywords: die-off coefficient; enterococci; karst; aquifer; fractures; channels; matrix

1. Introduction

Presence of enterococci in the pumping sites for drinking water supply of Bokanjac–Poličnik karst aquifer is an indicator of faecal pollution which is very dangerous for the environment and people living in that area. The Bokanjac–Poličnik aquifer is burdened by pollution caused by seepage of polluted water from the surface (septic tanks). The die-off coefficient of faecal indicator bacteria, such as enterococci (ENT), in typical conditions of groundwater flow through the karst aquifer (fracture porosity) is unknown. The objective of this study is to define appropriate methodology for determining the die-off coefficient of faecal indicator bacteria, ENT, when transported in a karst environment. Besides that, additional goals are to determine self-purification capacity (sorption and die-off expressed with associated coefficients) in case of incident events or continuous pollution processes and to determine the dominant process in removal of ENT in the observed karst environment. The proposed

methodology strives to cope with limited amount of available hydrological, hydrogeological and biochemical data on the analysed karst aquifer.

Karst aquifers are formed in a soluble rock, usually limestone, and they are characterised by distinctive heterogeneity in a sense of structure and indentedness of rock mass, the so-called matrix, inside which one could find different karst phenomena such as karst sinkholes, springs, caverns, fractures and caves. Over the years, many researchers dealt with the conceptual solutions and the idea of structural schema of karst [1–5]. In general, a karst system could be divided into four subsystems:

1. Soil: surface, infiltration part over which aquifer is water-supplied—water recharge can be autogenous, allogeneic, diffuse or concentrated, depending on the characteristics of the surface layer.
2. Epikarst: subsurface layer which stores part of the infiltrated water; it accepts the water which is drained through the vertical flow in a unsaturated zone.
3. Vadose zone: connects subsurface layers with a saturated zone;
4. Saturated zone: it consists of a low permeable matrix and a net of highly permeable karst channels and fractures.

In a karst environment, groundwater flow is mostly conducted through fractures and karst channels where quite high flow velocities can be achieved. Although the matrix can be very porous due to small primary permeability, it has no contribution to the flow to a large extent, which is why diffuse flow happening inside of it, is often neglected. On the other hand, the retention capacity of the matrix is quite big and inside its huge amounts of water can be stored; that water is gradually seeped towards springs, fractures and karst channels. Therefore, karst rock and aquifer are characterised by triple porosity (the matrix, fractures, karst channels), laminarly-diffuse flow inside the matrix and turbulent flow inside the karst channels and fractures.

Different types of mathematical and numerical models could be applied to deal with hydrological and ecological problems of karst aquifers with dual and/or triple porosity depending on available data and identified problems. Distributed parameter models are often applied to systems of karst aquifers [6–9]. Those types of models are usually applied to places where enough data about the features of aquifer is gathered. Those features include permeable and non-permeable boundaries, zones of inter-layer seepage, positions of faults, springs and sinks. Distributed parameter models require division of the aquifer into small representative three-dimensional volumes such as finite difference cells, or finite element cells. Basic hydraulic features of aquifer (hydraulic permeability, transmissivity, storage, effective and total porosity) are spaced and can be distinguished and changed for every model cell or element. Various numerical strategies have been used in karst aquifers analysis over the years. The simplest approach is the one which assumes that karst aquifer conducts oneself equivalently towards the medium of intergranular porosity in the conditions of flow and transport. The approach is called single continuum porous equivalent (SCPE) model. SCPE is based on the acquisition of the continuum scheme and flow simulation by the potential flow equation, and the model itself simulates laminar flow. Relevant research in [10–16] are just a few examples of successful implementations of the SCPE approach when it comes to researches of water resource. The approach is based on the fact that higher values of hydraulic conductivity are given to the model cells for which it is known or assumed that go through the fractures compared to the surrounding cells which therefore represent a weakly permeable matrix. Computer codes mostly used are different variants of the MODFLOW software.

The research which dealt with controlled discharge of sewage water from septic tanks showed the importance of enough thickness of the unsaturated zone. It also showed that the concentration of the faecal indicator bacteria is largely decreased with the flow heading towards the depth [17,18]. However, the research also indicated that the transport of the bacteria through the soil intensified due to more pronounced precipitation, and the increased concentration of bacteria on the pumping sites coincided with the periods of intensive precipitation [19,20]. In case that bacteria reach the

saturated zone relatively quickly and in high concentration, it will represent danger for the ecosystem in which they are found. Several studies [21–25] have shown that the microorganisms and colloids can easily be transported by preferential flows. Firouzi et al. [26] analysed transport and bacteria removal in a limestone soil under the saturated conditions. He noticed that the breach of bacteria mass is enlarged with the increase of velocity of groundwater flow. Potential presence of pathogens in groundwater could be discovered by monitoring the presence of faecal indicator bacteria such as ENT. A general model of bacteria transport consists of advection, dispersion and the process of attachment (sorption), detachment (desorption), filtration, blocking, die-off in contact with the porous medium and die-off in a liquid phase [27]. A high rate of attachment and removal of bacteria on limestone grounds could be ascribed primarily to the fact that calcium carbonate is mostly positively charged when in neutral pH level surroundings which makes it convenient for the attachment of negatively charged bacteria. According to [27], blockage and detachment do not have a significant effect on bacteria transport, and the most plausible reason is the die-off that is happening on the surface of particles, that again enables the particle surface to be free for attachment. The bacterial die-off rate in a liquid phase is under the influence of factors such as temperature, light, pH level, amount of poisoned substances, dissolved oxygen and protozoa. The die-off coefficients, k, of the faecal indicator bacteria are defined mainly for the conditions of flow through the aquifer with the intergranular porosity, and with somewhat different values depending on all the above-mentioned factors [28–30]. One of the most important factors that affect die-off of the bacteria is the temperature. John and Rose [31] compared approximately ten studies which dealt with the investigation of the die-off of the Escherichia coli (EC) and ENT in a temperature range from 3 to 37 °C. In a total sample of 35 values, the die-off coefficient of the EC varies from 0.01 to 1.5 day^{-1}. Higher levels of die-off (above 0.5 day^{-1}) is noticed with temperatures above 20 °C. According to [27], despite heterogeneous conditions during different experiments, from the gathered data, it can be concluded that the value of the die-off coefficient increases with the temperature rise. The average die-off coefficient value with the temperature of 10 °C is 0.15 day^{-1} that is 0.5 day^{-1} with the temperature of 20 °C. Impact of the soil to the die-off rate depends primarily on the local conditions on the catchment, and the effect can be positive or negative which depends on the presence of nutrients, toxic substance, oxygen, etc. Heavy metals have toxic impact on bacteria and with its presence in ground water and soil, die-off level is increased [32,33]. The level of die-off of the faecal indicator bacteria in oxygen-saturated water is significantly lower in relation to water with low oxygen saturation [32].

Based on the above mentioned, one can conclude that the chances for the bacteria removal in karst channels are very small due to preferential flows and high velocities of the groundwater found inside of them. Mechanisms of bacteria removal from water are conducted by percolation through the surface layer, epikarst and unsaturated zone of karst rock where soil pores and percolation velocities are significantly lower in relation to karst channels. Furthermore, it is determined that intensive precipitation can trigger a major flow of water through the epikarst by virtue of binding smaller fractures and creating a continuous flow. In such conditions, hydraulic pressure can mobilise water stored inside an epikarst towards larger fractures, and eventually saturated zone. Such a flow concept is called piston-type flow [34]. Schwarz et al. [34] noticed that the largest number of bacteria reaches the saturated zone shortly after intensive precipitation. The phenomenon is also explained because of smaller fractures binding inside the epikarst and moving of the bacteria sedimented within it. Williams [35] also recognised the piston-type flows when he noticed that the concentration of pollution passing through the epikarst zone exponentially decreases over time. Concentration of the bacteria can be increased with the emergence of "new" precipitation (so-called "pulse" effect). That is why each precipitation can be looked at as a separate event, i.e., as an impulse that triggers pollution towards the saturated zone.

2. Study Site

The Dinaric karst in Croatia, globally known as "locus typicus" of karst landscapes, is characterised by very irregular karstification which is caused by tectonics, compression, reverse faults and over thrusting structures. The research area is generally located between the Adriatic microplate to the southwest and the Dinaric regional structural unit to the northeast. Their contact is represented by reverse faults that strike northeast-southwest [36]. Eocene and Cretaceous limestone is a main component of the terrain [37,38]. Carbonate rocks, clastic rocks and quaternary soil are basic rock masses that build the terrain. The most represented rock from those three is the most permeable one, the limestone. The whole hydrogeological system of Bokanjac–Poličnik covers an area of 235.7 km². The Bokanjac–Poličnik aquifer takes around 86% of the Bokanjac–Poličnik catchment, and it spreads around the carbonate rocks formation. The remaining part, around 33 km² belongs mainly to non-permeable flysch surfaces [39].

Stratigraphically, the upper zone of the terrain is shallow and highly karstified, while the deeper zone is characterised as a low permeability rock mass, with a network of karst fractures [40]. Typical karst shapes in the analysed area are not particularly developed and the most important objects in the hydrogeological sense are active sinks. The most important sink is in Biljane Donje where tracer tests were carried out and where underground connection with the spring Golubinka was proven. It was there that the highest groundwater velocity was measured with apparent values of 8.1 cm/s [41]. The flow direction goes from the mid and eastern parts of the catchment towards the shore. The flow begins on the higher parts of the relief, parts of Biljane Donje from where water flows towards northwest, and in that way, it forms the Oko spring. In cases of high waters, the water rises from the Oko spring and forms surface flow called Miljašić Jaruga. The flow then continues towards the Boljkovac and Golubinka springs, and due to "hanging" and complete barriers, part of the water is filtrated south towards Bokanjačko blato and Jezerce well. The tracer tests in the area conducted in 2007 [39] suggests that apparent flow velocities, in the periods of hydrologically low groundwater levels (dry season), are very low compared to other karst terrains. In the periods of low groundwater level, in that morphologically low terrain, gradients are extremely small and water flows extremely slowly. That is why in such dry periods, the groundwater level in wells is rather low, but the inflows are still continuous, and with specific capacity decrease, it can always pump ten to twenty litres per second of the groundwater. Today, for the purpose of water supply, six wells are used. According to the information of municipal corporation in Zadar not a single settlement in the hinterland of Zadar has public sewage system and waste water from the households is treated in septic tanks. Such a way of dealing with waste water presents danger from polluting hydrogeological system Bokanjac–Poličnik and the springs within it.

The data on groundwater levels and concentrations of ENT on the wells in Jezerce and B4 were gathered for the period of 1 January 2012–19 October 2016. Based on [42], an insight was given into the values of the hydraulic conductivity *K* at the depths from 20 to 50 meters on several locations on the catchment (Figure 1, purple dots). The groundwater level data for that period (1 November 1966–31 June 1967) were also gathered (Figure 1, red dots).
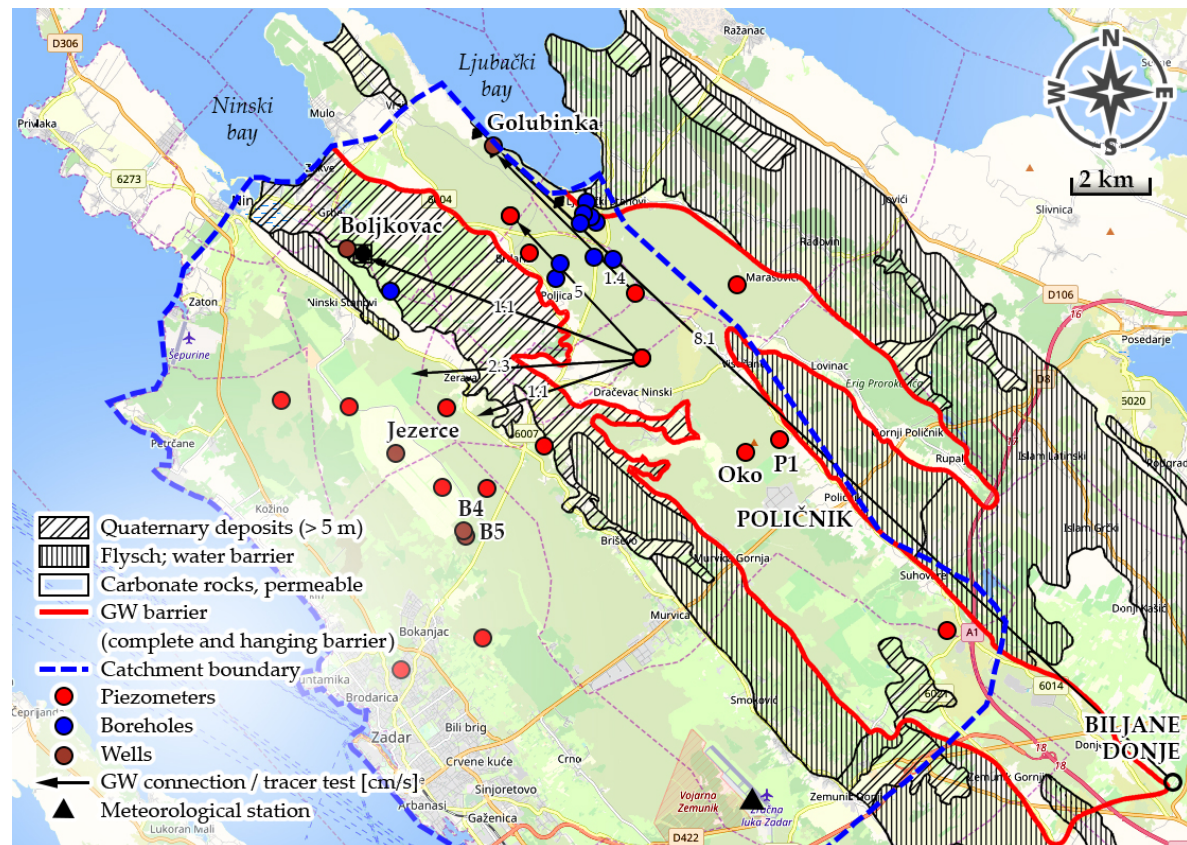
Figure 1. Schematic hydrogeological map of the Bokanjac-Poličnik catchment area with the locations of boreholes, piezometers, wells and groundwater barriers.

3. Materials and Methods

The suggested methodology for determining the die-off coefficient of the enterococci in the conditions of transport through the karst aquifer consists of two basic steps (Figure 2). Preliminary analysis, as the initial step of the methodology, serves for making specific assumptions regarding detection of what triggers enlarged ENT concentrations on the analysed wells, as well as regarding potential source of pollution. Information from the preliminary analysis were a basis for making an analytical transport model which is the second step and the backbone of the suggested methodology. The goal of the analytical model was to determine the dominant factor in the process of natural removal of ENT by transportation through a karst catchment. The model consists of two parts of the pollution transport process. The result of the first part (vertical component of the flow) was the value of ENT concentration at the end of the unsaturated zone, C_{VAD}. In the second part, based on the known ENT concentration in the wells, by inverse procedure, the value of ENT concentration at the beginning of horizontal flow part (C_{SAT}) was calculated.
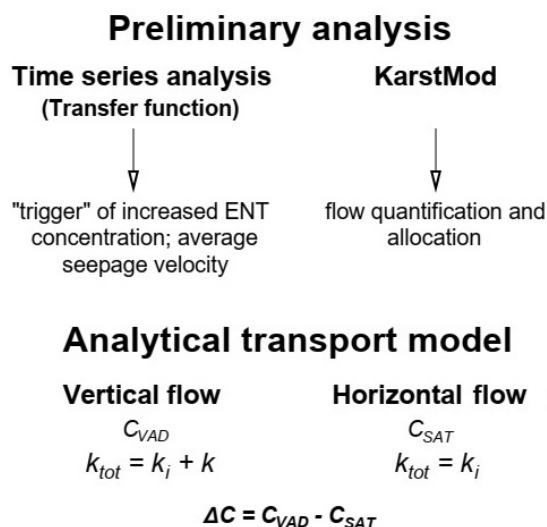
Preliminary analysis

Time series analysis
(Transfer function)

KarstMod

"trigger" of increased ENT
concentration; average
seepage velocity

flow quantification and
allocation

Analytical transport model

Vertical flow

C_{VAD}

$k_{tot} = k_i + k$

Horizontal flow

C_{SAT}

$k_{tot} = k_i$

$\Delta C = C_{VAD} - C_{SAT}$

Figure 2. Basic steps of the proposed methodology for determining the die-off coefficient (k_{tot}—total die-off coefficient, k_i—natural die-off coefficient, k—sorption coefficient).

3.1. Preliminary Analysis

3.1.1. Time Series Analysis—Transfer Function

Preliminary analysis primarily dealt with the statistical analysis of the gathered data regarding the precipitation, groundwater levels in Jezerce and B4 wells, pumping rates and ENT concentration for the period from 1 January 2012–19 October 2016 at Jezerce and B4 wells. The goal was to determine the correlation strength between the above-mentioned parameters. The model that best describes the relation between input (precipitation, pumping and levels) and output (concentration of enterococci) is defined by the time series analysis. Interpretation of results gave an insight into the dominant variable (precipitation, pumping or levels) which affects the enlarged concentration of ENT on the pumping sites, as well as the approximate reply time of the concentration increase depending on input variables.

A transfer function was used as a method for data analysis, as well as the CAPTAIN Toolbox [43–45] integrated in the MATLAB. The transfer function can serve as an effective tool when defining structure and nature of the mathematical models of hydrological systems by using sophisticated statistical methods and interpreting model equations in the field of physics. In statistics, transfer function modelling belongs to the field of time series analysis [44,46] and includes identification and evaluation of model via time series data. The identification of time series data relates to defining the most suitable model structure, i.e., triad values *n*, *m* and *δ*. Parameters *n*, *m* and *δ* can be seen in the Equation (1). Refined instrumental variable algorithms offer a possibility of simple analysis, so-called SISO analyses (one input, one output), but also the complex analysis in a sense of two and more inputs and one output, so-called MISO analyses. Based on the transfer function, it is possible to define time detachment of increased concentrations depending on the initial impulse with a goal to define average time of seepage from potential sources of pollution to the wells.

A simple SISO model can be described by Equation (1) or by a transfer function, Equation (2) [46]:

$$y_t + a_1 \cdot y_{t-1} + a_n \cdot y_{t-n} = b_0 \cdot x_t + b_1 \cdot x_{t-1-\delta} + b_m \cdot x_{t-m-\delta} + N_t \tag{1}$$

$$y_t = \frac{B(L)}{A(L)} \cdot x_{t-\delta} + \frac{1}{C(L)} \cdot e_t, \tag{2}$$

where y_t is the output from the linear model at time *t*, x_i is input into the model in time *t*, δ is the time delay of the input according to the time *t*, N_t is the value of a correlated random variable at time *t*,

e_t value of a random variable with standard distribution with zero average and constant scatter at time t.

The user defines the triad n, m and δ, and the algorithm chooses and presents the best possible solutions depending on the chosen identification criterion (YIC, RT2, AIC or EVN). The software offers the possibility of graphic interpretation of results through a graphical user interface where the 20 best solutions are generated according to chosen criteria, and all with the purpose of simplifying identification procedure.

The MISO transfer function, suitable for determining the input parameter with dominant influence on the output, in discrete form is expressed as:

$$y_t = \frac{B_1(z^{-1})}{A(z^{-1})} \cdot u_{1,t} + \cdots + \frac{B_m(z^{-1})}{A(z^{-1})} \cdot u_{m,t}, \tag{3}$$

where m is the number of input variables that is assumed to influence the output, and A and B_i represent polynomials. SISO and MISO analyses were made on the data sets from the Jezerce and B4 wells.

3.1.2. Quantification of the Groundwater Flow Distribution

The numerical model KarstMod was used to estimate the distribution of total seepage through the karst aquifer on the fracture flow (karst channels and fractures) and diffuse flow (matrix). The catchment area of the Golubinka spring was taken into consideration in this step of the preliminary analysis. The quantification of the fracture and diffuse flow component was performed based on the well-known discharge hydrograph from the Golubinka spring and the precipitation data (mm/day) for the period 1 January 2012–31 December 2015.

KarstMod is a platform for the simulation of the precipitation-discharge ratio of the karst springs and the analysis of the hydrodynamic characteristics of the karst aquifer. By defining model structure and its fluxes (precipitation, evapotranspiration, pumping rates in the components), warm-up, calibration and validation periods, an optimal model parameter set can be obtained as the model output. The optimisation parameters of the model and the range of their values are shown in Table 3, together with the adopted optimal values used in the calculation of discharge hydrograph. The two-level structure, with three compartments constitutes the model (Figure 3). Compartment E (epikarst) represents the higher level, while compartments M (matrix) and F (fractures) represent the lower level. It is assumed that the components M and F are filled from the higher-level E and that the main quantities of flow will occur through the fractures (Q_{FS}). The model has three water balance equations [47]:

$$\frac{dE}{dt} = P_{eff} - Q_{EM} - Q_{EF}$$
$$\frac{dM}{dt} = Q_{EM} - Q_{MS} - Q_{MF} \tag{4}$$
$$\frac{dF}{dt} = Q_{EF} - Q_{FS},$$

where E, M and F are water levels in compartments E, M and F respectively, S is the outlet of the system, P_{eff} is the effective precipitation, assumed as $0.6 \cdot P$ [48], and Q_{EM}, Q_{EF}, Q_{MS}, Q_{FS}, Q_{MF} are internal discharge rates per unit surface area.
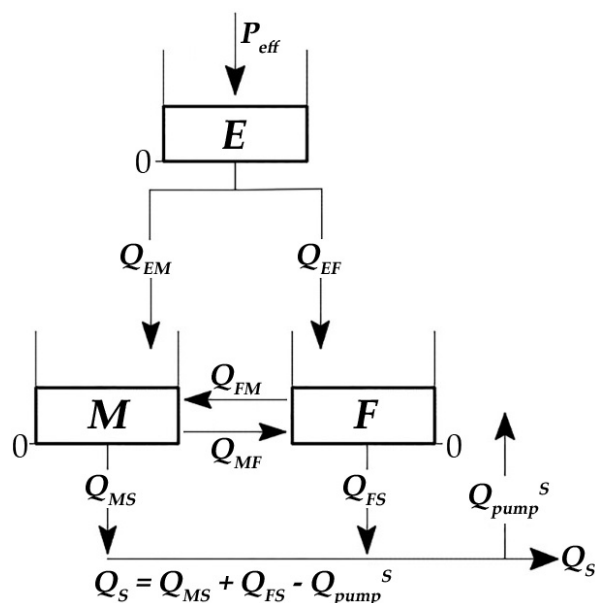
Figure 3. Structure of the KarstMod model platform.

The 90-day period (1 January 2012–31 March 2012) was used as the warm-up period and these results were not used for the model calibration. For the calibration, 1004 days were used (1 April 2012–31 December 2014) for which the optimum model parameter set was obtained. For the model validation, the year 2015 was used. Model performance was tested by using the Nash–Sutcliffe efficiency coefficient (*NSE*) and the modified Balance Error (*BE*).

Information regarding flow distribution inside the karst aquifer was used to create numerical flow and transport model within software MODFLOW. The numerical strategy SCPE was used for flow simulation. The examination was done here on how numerical model reacts on the distribution of flow onto diffuse flow and fracture flow. Cells which are given relatively high value of hydraulic conductivity represent fractures, while the surrounding cells represent the matrix, and they are given significantly lower values of hydraulic conductivity coefficient. The concept can be visualized as an extremely permeable karst channel (fractures) immersed into a low permeable net called the matrix. For the purpose of checking the flow distribution given by KarstMod, a numerical model of Golubinka catchment was created (Figure 4) with the cell dimensions of 200 × 200 m horizontally, and with two layers vertically. The bottom layer was 1 m thick (−2 to −1 m a.s.l.), and the top layer was 61 m (−1 to 60 m a.s.l.). Slow, diffuse flow took place in the top layer while more significant seepage took place in the bottom layer, where fractures and karst channels were simulated by setting higher values of hydraulic conductivity. Model parametrization in a sense of hydraulic conductivity K_x, K_y, K_z, effective porosity n_{eff} and total porosity n_{tot} (Table 1) was adopted based on the calibration procedure in [49].

Table 1. Adopted model parameters based on the calibration procedure.

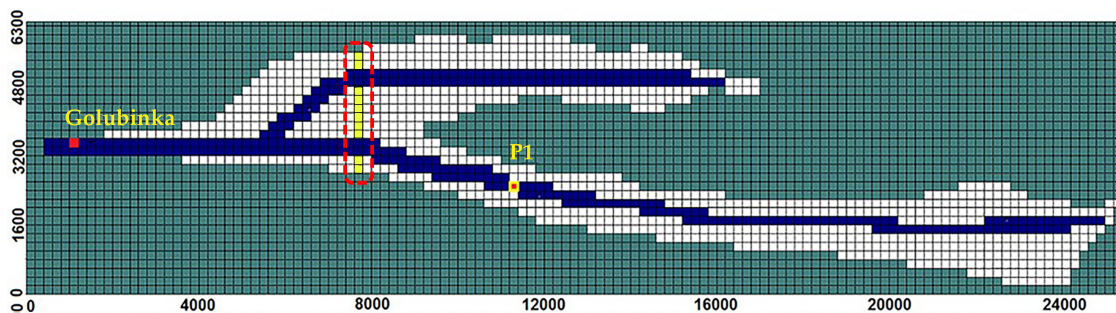| Parameter	Upper Layer	Lower Layer
K_x (m/s)	$1 \cdot 10^{-4}$	$3 \cdot 10^{-1}$ / $1 \cdot 10^{-4}$
K_y (m/s)	$1 \cdot 10^{-4}$	$3 \cdot 10^{-1}$ / $1 \cdot 10^{-4}$
K_z (m/s)	$1 \cdot 10^{-4}$	$3 \cdot 10^{-1}$ / $1 \cdot 10^{-4}$
n_{eff} (−)	0.02	0.01
n_{tot} (−)	0.02	0.02

Figure 4. Spatial distribution of hydraulic conductivity coefficients K_x, K_y, K_z in the bottom layer (from -2 to -1 m a.s.l.) with the marked section for flow distribution control and boundary conditions (Golubinka and P1). Blue area indicates the values K_x, K_y, $K_z = 3.0 \cdot 10^{-1}$, and the white area indicates the values K_x, K_y, $K_z = 1.0 \cdot 10^{-4}$.

3.2. Analytical Model

The analytical model integrated two parts of a pollution transport process (Figure 5); the first part with the percolation from the septic tanks to a saturated zone, and the second part in which horizontal flow and transport were followed inside of the saturated zone.
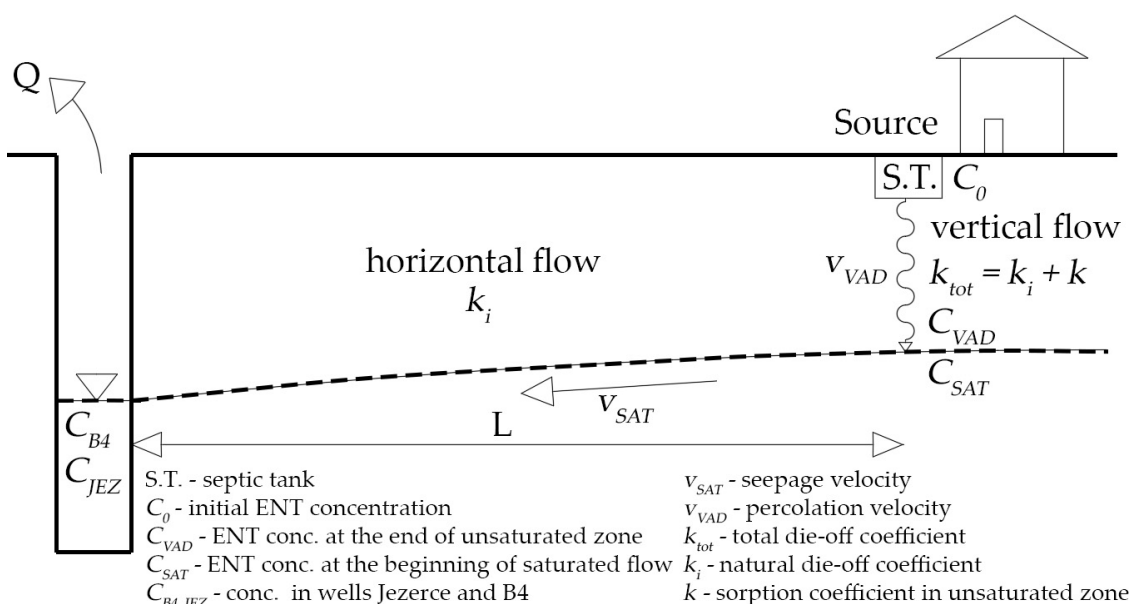

Figure 5. The scheme of the analytical transport model.

Input data in the implemented analytical transport model were measured groundwater levels on the wells B4 and Jezerce, measured ENT concentration, surface elevation, and data regarding the distance between suspicious pollution sources from the wells Jezerce and B4. For the initial ENT concentration around septic tanks, the value of $4 \cdot 10^8$ cfu/100 mL was adopted (this value has been verified by an authorized laboratory). The calculation was conducted through following steps:

(a)　Transport through the unsaturated zone (vertical flow)—calculation of the ENT concentration at the end of the unsaturated zone C_{VAD} (the place of shift from vertical to horizontal flow);

(b)　Transport through the saturated zone (horizontal flow)—calculation of the ENT concentration C_{SAT} at the beginning of the horizontal flow route (inverse procedure) based on measured concentration C_{B4} and C_{JEZ} on the wells B4 and Jezerce.

The calculation was done for each of the suspicious pollution sources and assumed flow directions (Figure 6) with the variation of the parameter-coefficient values in a transport model (die-off and

sorption coefficients, turbulent filtration coefficeint, etc.). The transport model parameters/coefficients were varied with the goal to achieve the minimum difference in concentrations $\Delta C = C_{VAD} - C_{SAT}$. Established statistical criterion was the root mean square error (RMSE). MATLAB was used for the implementation of the calculation.
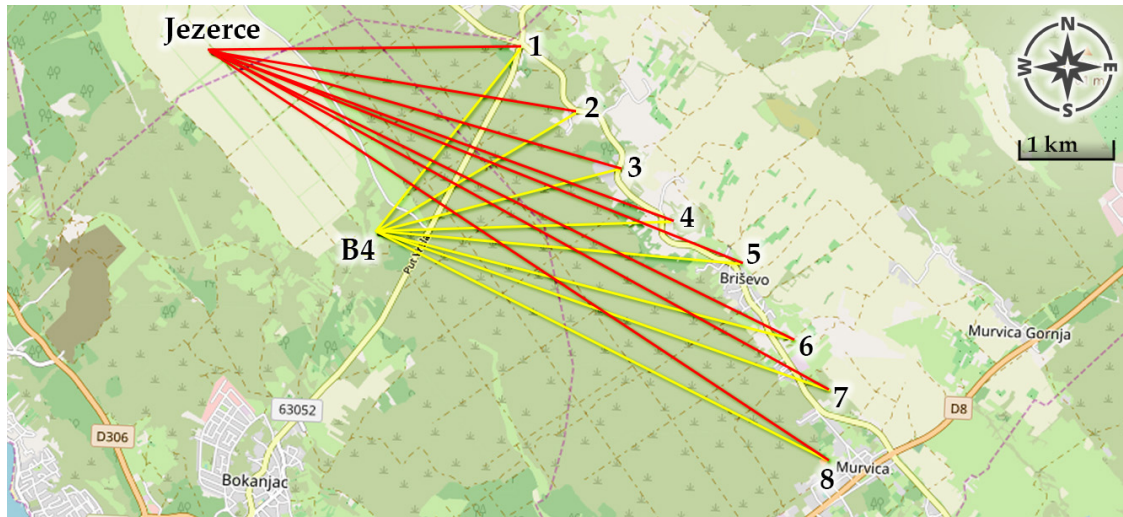

Figure 6. The location of the pollution source in relation to the wells Jezerce and B4 along with possible flow paths.

3.2.1. Vertical Flow

The ENT concentration at the end of the vertical flow section C_{VAD} was calculated according to Equation (5):

$$C_{VAD} = T \cdot C_0 \cdot e^{-k_{tot} \cdot t_p} \tag{5}$$

$$k_{tot} = k_i + k \tag{6}$$

$$t_p = \frac{d}{v_{VAD}/R}, \tag{7}$$

where C_0 is the initial ENT concentration ($4 \cdot 10^8$ cfu/100 mL), T is the on/off function of initial humidity, t_p is the percolation time, k_{tot} is the total die-off coefficient, k_i is the natural die-off coefficient, k is the sorption coefficient, d is the depth of the unsaturated zone, v_{VAD} is the percolation velocity, and R is the retardation.

The on/off function of the initial humidity T considers the impact of the previous precipitation on the wettability of the porous medium, thus ensuring a more pronounced seepage velocity. The parameter T was introduced to cancel the impact of precipitation on the pollution transport after a longer drying season, when subsurface conditions were not suitable for the infiltration and percolation process. The value of the on/off function of the initial humidity was determined according to the following criterion:

$$T = \begin{cases} 0 & \text{if} \quad P_i + P_{i-1} + P_{i-2} < P_{mean(1/1/2012-19/10/2016)} \\ 1 & \text{if} \quad P_i + P_{i-1} + P_{i-2} > P_{mean(1/1/2012-19/10/2016)} \end{cases}, \tag{8}$$

where P_i is the precipitation height in the analysed week, P_{i-1} is the precipitation height of $i-1$ of the analysed week, P_{i-2} is the precipitation height of $i-2$ of the analysed week, P_{mean} is the average precipitation amount for the analysed period of 1 January 2012–19 October 2016.

The seepage velocity in the horizontal flow section (v_{SAT}) was obtained by applying the nonlinear seepage law [50]:

$$v_{SAT} = K \cdot \sqrt{\frac{h_{B4} - h_{Jezerce}}{L}}, \qquad (9)$$

where v_{SAT} is seepage velocity, K is the turbulent filtration coefficient, L is the length of the horizontal section of the flow.

The impact of previous precipitation on the value of the ENT concentration is considered through modification of the Equation (5), so the final ENT concentration at the end of an unsaturated zone $C_{VAD,i}$ was calculated by using the following equation:

$$C_{VAD,i} = T \cdot C_0 \cdot e^{-k_{tot} \cdot tp} + C_{VAD,(i-1)} \cdot F_1 + C_{VAD,(i-2)} \cdot F_2, \qquad (10)$$

where $C_{VAD,i}$ is the ENT concentration at the end of the unsaturated zone, $C_{VAD,(i-1)}$ is the ENT concentration at the end of the unsaturated zone for $i-1$ of the analysed week, $C_{VAD,(i-2)}$ is the ENT concentration at the end of the unsaturated zone for $i-2$ of the analysed week, F_1 and F_2 are the coefficients of the delayed concentration.

The second and the third member on the right side of Equation (10) refer to the delayed concentration, i.e., the one that is left behind in unsaturated zone. They depend on catchment conditions, i.e., seepage velocity and travel time from the pollution source to the wells B4 or Jezerce. F_1 and F_2 are also calibrated and optimised parameters with the possible values expressed hereafter:

$$F_1 = \begin{cases} 0 & \text{if} \quad t_s < 7 \text{ days} \\ 0.2 - 0.5 & \text{if} \quad 7 \text{ days} < t_s < 14 \text{ days} \\ 0 & \text{if} \quad 14 \text{ days} < t_s < 21 \text{ days} \end{cases} \qquad (11)$$

$$F_2 = \begin{cases} 0 & \text{if} \quad t_s < 7 \text{ days} \\ 0 & \text{if} \quad 7 \text{ days} < t_s < 14 \text{ days} \\ 0.05 - 0.2 & \text{if} \quad 14 \text{ days} < t_s < 21 \text{ days} \end{cases}, \qquad (12)$$

where t_S is the seepage time in the saturated zone.

3.2.2. Horizontal Flow

The aim of this part of the model is to calculate ENT concentration at the beginning of the horizontal part of the flow C_{SAT} (Equation (13)), based on the measured values of concentration on the wells Jezerce and B4.

$$C_{SAT} = \frac{C_{B4} \text{ or } C_{JEZ}}{e^{-k_i \cdot t_s}}, \qquad (13)$$

where C_{B4} or C_{JEZ} are measured ENT concentrations on wells B4 and Jezerce. The value of the k_i is equal to the value of the die-off coefficient in the Equation (6).

Seepage time in the saturated section of the flow is calculated using the following equation:

$$t_s = \frac{L}{v_{SAT}}. \qquad (14)$$

It should be mentioned that the calculation was applied only in cases when the condition of total time of seepage through the karst medium was satisfied in the following way: $t_s + t_p < 7$ days (time from the initial rain impulse to the end of flow through horizontal part of the flow is less than seven days). If it is the opposite way, the concentration in an observed time is zero and it is eliminated from further calculation.

　　　The time limitation was established because of maximal correlation strength accomplished while adopting seven days lag between precipitation occurrence and increased ENT concentration on wells (from the time series analysis). Delayed concentration in the unsaturated zone were considered through adequate members in the Equation (10).

4. Results

4.1. Preliminary Analysis

4.1.1. Time Series Analysis—Transfer Function

　　　Three SISO analyses (precipitation/groundwater levels/pumping rate—ENT concentrations) and one MISO analysis (precipitation/ groundwater levels—ENT concentrations) for Jezerce and B4 were made. From the results of the SISO analysis (Figure 7) it is evident that precipitation have the greatest impact on the increased ENT concentration in the wells. Optimal values of *n*, *m* and *δ* as well as the value of the identification factor are shown in Table 2. The results represent the best compromise between the identification criterion RT2 and YIC. The analysis shows that the most pronounced correlation strength between precipitation and concentration is obtained for the time lag *δ* = 5 days for the B4 and seven days for the Jezerce well. This value corresponded to the velocity of the groundwater flow of 1–3 cm/s from the Poljica, Poličnik, Visočane, Briševo settlements to the wells B4 and Jezerce, obtained with the tracer tests [40]. These settlements were taken into consideration in the further implementation of the methodology. In Figure 8, the results set of SISO and MISO analysis is shown, together with the measured ENT concentrations.

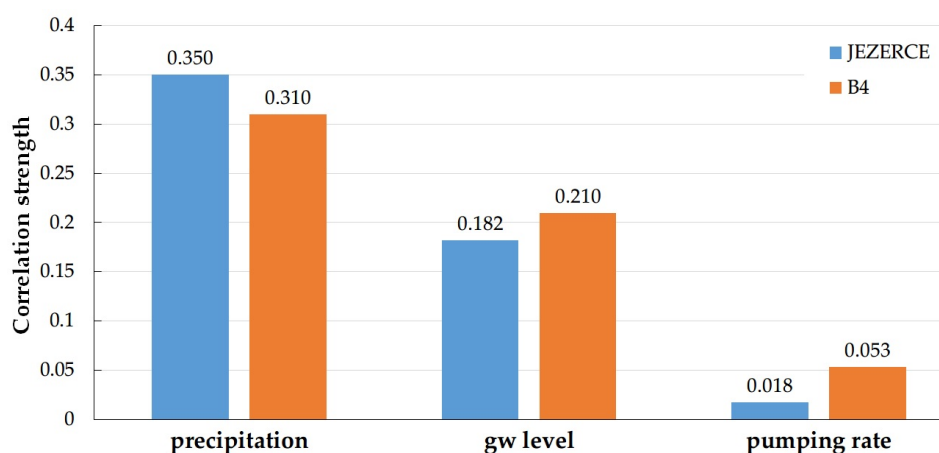**Figure 7.** One input, one output simple analysis (SISO) analysis of the input data and enterococci (ENT) for wells B4 and Jezerce.
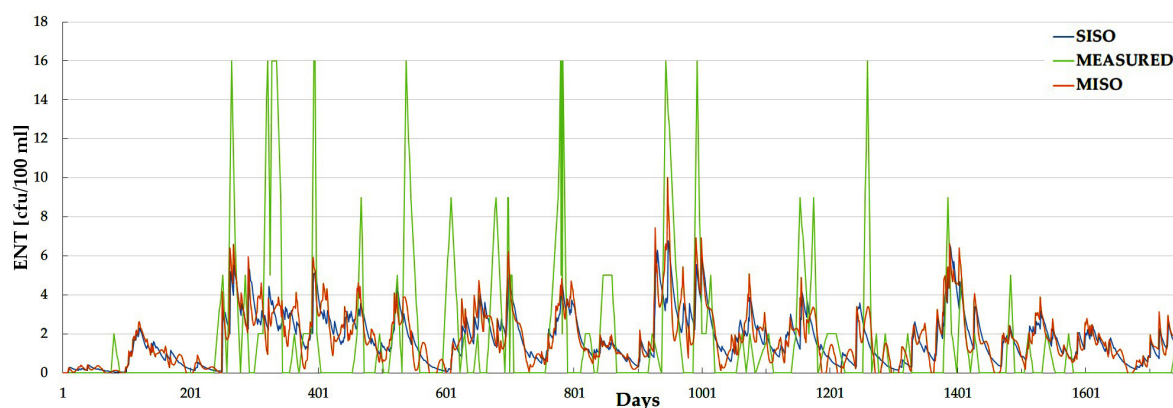

Figure 8. Results of SISO and two and more inputs, one output complex analysis (MISO) for the Jezerce well.

Table 2. Model structure and values of the identification factors.

WELL	STRUCTURE	SISO		MISO	
	$(n\ m\ \delta)$	RT2	YIC	RT2	YIC
JEZERCE	1 1 **7**	0.35	−5.23	0.396	−0.05
B4	3 2 **5**	0.31	−1.61	0.353	−1.35

4.1.2. Quantification of the Groundwater Flow Distribution (KarstMod)

The calculated discharge hydrograph and the results of flow distribution calculation, obtained based on the optimal parameters from Table 3, are shown in Figures 9 and 10. According to the results of the model, 19% of the total flow took place in the diffuse phase (matrix) and 81% in the fracture component of the flow (fractures and karst channels).

For the control of the flow distribution in MODFLOW, the cross section marked in Figure 4 was taken into consideration. Yellow cells represent the matrix (K_x, K_y, $K_z = 1 \cdot 10^{-4}$), and blue cells represent karst channels, i.e., fractures (K_x, K_y, $K_z = 3 \cdot 10^{-1}$). In cross-sectional view, there were 14 cells altogether, 10 of which simulated the matrix. The average velocity inside of the matrix was $5 \cdot 10^{-5}$ m/s. Total flow per unit meter was estimated through the product of velocity and height of the water level inside of the cells and amounted 0.03 m³/s for seeping through the matrix. In the fractures (blue cells in Figure 4) the average velocity amounted to 0.042 m/s. Total flow per unit volume through fractures was 0.17 m³/s (velocity times cell height of 1 meter times number of cells). The given relation of total flow apportionment was 84% for seeping through channels and 16% of water which was seeped through low permeable matrix. Those results are in accordance with the results from KarstMod, and therefore the SCPE strategy can be applied in creating the numerical flow and transport model for the Bokanjac–Poličnik catchment.

Table 3. Ranges of parameter values carried out by the optimisation procedure based on the discharge hydrograph of Golubinka spring and the optimal values of the parameters used for calculating hydrograph with the KarstMod model

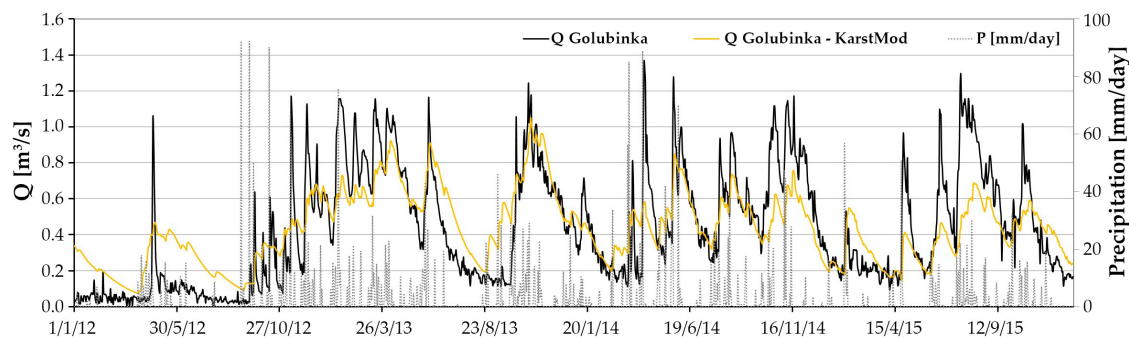| Optimisation Parameter	Range	Optimal Value
R (km²)	20–70	30.42
E (mm)	0–100	1.76
M (mm)	0–100	19.73
F (mm)	0–100	25.98
k_{EF} (mm/day)	$1 \cdot 10^{-4}$–100	0.0551
α_{EF} (−)	$0.2 \cdot 10^{-4}$	2.08
k_{EM} (mm/day)	$1 \cdot 10^{-4}$–100	0.0954
k_{MS} (mm/day)	$1 \cdot 10^{-4}$–100	0.013
k_{MF} (mm/day)	$1 \cdot 10^{-4}$–100	0.00026
k_{FS} (mm/day)	$1 \cdot 10^{-4}$–100	0.0277
α_{FS} (−)	0.2–4	1
WOBJ value (calibration stage)		0.61
WOBJ value (validation stage)		0.63

Figure 9. Discharge hydrograph of the Golubinka spring obtained by the KarstMod model simulation.
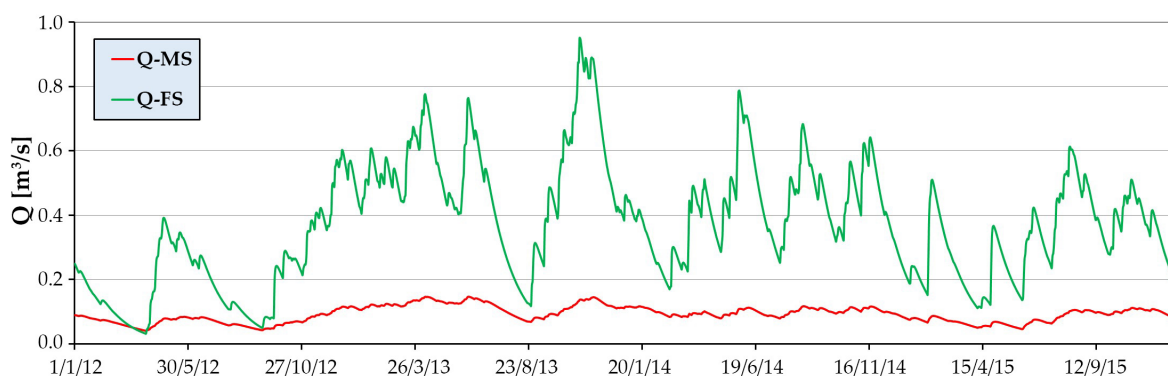

Figure 10. Flow distribution between the diffuse (MS) and the fracture (FS) flow components through the analysed karst aquifer.

4.2. Analytical Model

The value range of variable and fixed parameters that appear in Equations (5)–(14) were firstly defined (Table 4). Flow directions from Figure 4 (distances) and the initial ENT concentration around septic tanks ($4 \cdot 10^8$ cfu/100 mL) were fixed values. ENT concentrations in the Jezerce and B4 wells were obtained by measurement. Die-off coefficient k_i depends on water temperature and varies from 0.15 day^{-1} (10 °C) to 0.5 day^{-1} (20 °C) [27]. That was consistent with water temperature of the analysed aquifer over the year so the die-off coefficient k_i in the calculation was taken within the limits of those values, which means 0.15 in the winter period, 0.5 in the summer period, and linearly interpolated in between. Retardation coefficient for faecal indicator bacteria acquired values in a range from 3 to 10 [51], and within the analytical model represented the optimised parameter. When it comes to percolation velocity v_{VAD}, [35] recognised three phases of flow in the unsaturated zone; zone of rapid velocities from 0.5–2 cm/s, second phase with velocities from 10^{-2} cm/s and the third with velocities lower than 10^{-3} cm/s. Percolation velocity v_{VAD} was also an optimised parameter in the calculation. Sensitivity analysis on the statistical criterion RMSE for the variable ΔC was suggested because literature data of some parameters had a relatively wide value range. Such implementation was suggested with the aim to narrow the value range of certain parameters, and preferably, to fix the least sensible. After that, Monte–Carlo simulation was used to generate $3 \cdot 10^5$ combination of values of variable parameters, and then they were implemented in Equations (5)–(14). Then, the calculation $\Delta C = C_{VAD} - C_{SAT}$ was made within the simulation period of 1 January 2012–19 October 2016.

Table 4. The range of values of the variational and fixed parameters that appear in Equations (5)–(14).

Parameter	The Flow Part	Type	Interval
Turbulent filtration coefficient, K (m/s)	Horizontal flow, (Equation (9))	Variational	0.1–0.5
Percolation velocity, v_{VAD} (m/s)	Vertical flow (Equation (7))	Variational	10^{-2}–10^{-4}
Retardation coefficient, R (−)	Vertical flow (Equation (7))	Variational	3–9
Natural die-off coeff., k_i (day^{-1})	Horizontal and vertical flow, (Equations (6) and (13))	Fixed, (linearly interpolated)	0.15–0.5
Sorption coeff., k (day^{-1})	Vertical flow (Equation (6))	Variational	1–11
Coeff. of the delayed concentration F_1	Vertical flow (Equation (10))	Variational	0.2–0.5
Coeff. of the delayed concentration F_2	Vertical flow (Equation (10))	Variational	0.05–0.2

4.2.1. Sensitivity Analysis

Table 5 shows the results of the sensitivity analysis, i.e., the values of the variation and fixed parameters used later in the Monte Carlo analysis. Figures 11 and 12 show the results of the sensitivity analysis for parameter K and v_{VAD}.

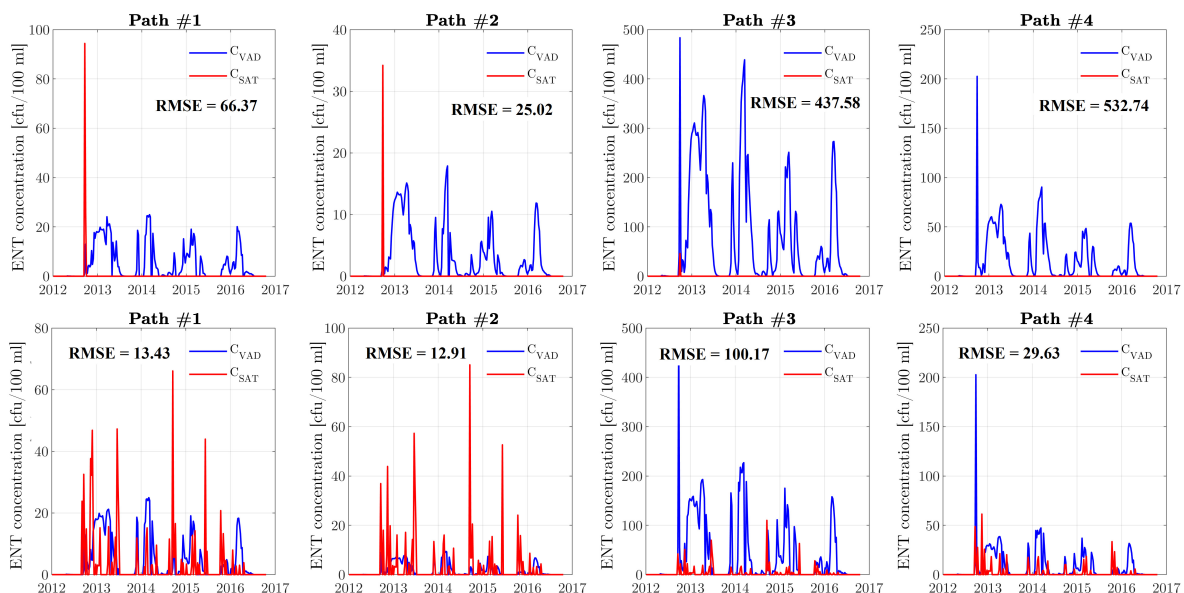**Figure 11.** The C_{VAD} and C_{SAT} concentration diagrams for flow paths 1–4 towards Jezerce well (from Figure 6) for $K = 0.2$ m/s (top 4 diagrams) and $K = 0.5$ m/s (bottom 4 diagrams).
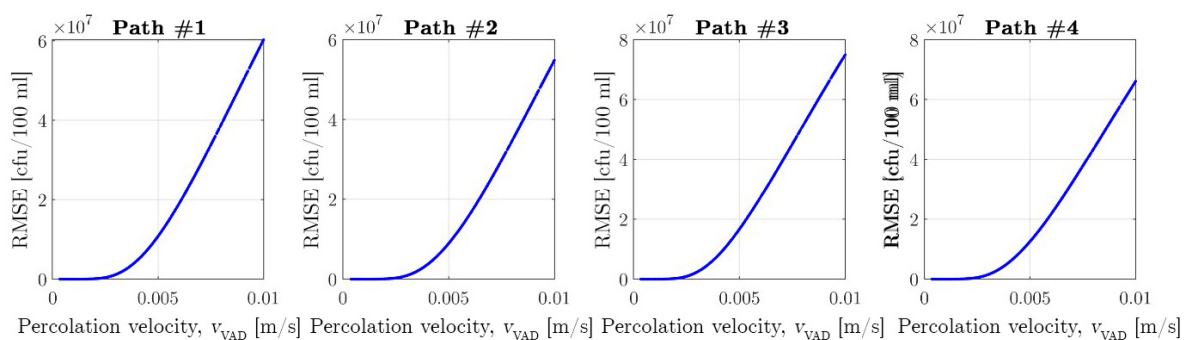

Figure 12. Sensitivity analysis based on root mean squared error (RMSE) (cfu/100 mL) for percolation velocity $v_{VAD} = 10^{-4}$ m/s − 10^{-2} m/s, for flow paths 1–4 towards the Jezerce well (from Figure 6).

Table 5. Values of variational and fixed parameters after the sensitivity analysis.

Parameter	Values
Turbulent filtration coefficient, K (m/s)	0.5
Percolation velocity, v_{VAD} (m/s)	$9 \cdot 10^{-4}$
Retardation coeff., R (−)	5–9
Natural die-off coeff., k_i (day^{-1})	0.15–0.5
Sorption coeff., k (day^{-1})	4–11
Coeff. of the delayed concentration F_1	0.5
Coeff. of the delayed concentration F_2	0.1

4.2.2. Monte–Carlo Simulations

Using the RMSE statistical criterion for variable ΔC, the optimal combination of the parameter values for each path 1–8 (Figure 6) was obtained (Tables 6 and 7). Figure 13 shows the calculated concentration of C_{VAD} and C_{SAT} for the paths 1 and 4 in the direction of the Jezerce well, gained with the adopted optimal parameters from Table 6. The Figure 13 shows that C_{VAD} and C_{SAT} concentrations are of the same magnitude and what is important, the pulse of the concentration occurrence appears to be the same for both phases of the transport, i.e., there was no delay in the concentration appearance in relation to each other.

Table 6. Optimal combinations of the variation parameters values with the respective RMSE for each path 1–8 towards Jezerce well.

Source	1	2	3	4	5	6	7	8
RMSE (cfu/100 mL)	10.85	12.66	15.1	9.77	11.7	19.87	21.91	23.58
K (m/s)	0.5	0.5	0.5	0.5	0.5	0.5	0.5	0.5
v_{VAD} (m/s)	$9 \cdot 10^{-4}$	$9 \cdot 10^{-4}$	$9 \cdot 10^{-4}$	$9 \cdot 10^{-4}$	$9 \cdot 10^{-4}$	$9 \cdot 10^{-4}$	$9 \cdot 10^{-4}$	$9 \cdot 10^{-4}$
R (−)	5.15	8.53	8.75	8.45	5.35	7.77	5.72	6.04
k (day^{-1})	11	7.9	7.7	8.2	8.4	7.5	7.8	7.5
F_1 (−)	0.5	0.5	0.5	0.5	0.5	0.5	0.5	0.5
F_2 (−)	0.1	0.1	0.1	0.1	0.1	0.1	0.1	0.1

Table 7. Optimal combinations of the variation parameters values with the respective RMSE for each path 1–8 towards B4 well.

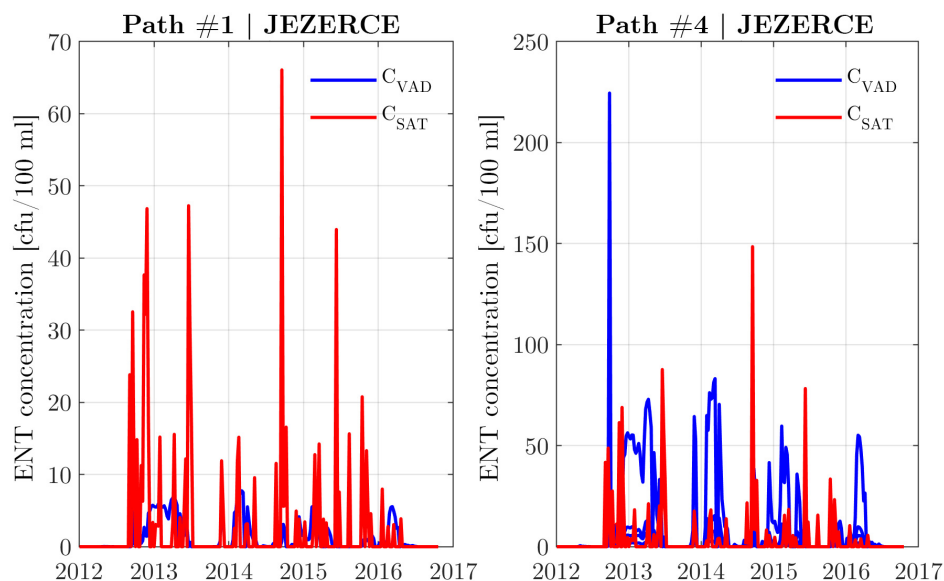| Source	1	2	3	4	5	6	7	8
RMSE (cfu/100 mL)	17.55	15.24	17.57	18.95	16.21	16.71	0	0
K (m/s)	0.5	0.5	0.5	0.5	0.5	0.5	0.5	0.5
v_{VAD} (m/s)	$9 \cdot 10^{-4}$	$9 \cdot 10^{-4}$	$9 \cdot 10^{-4}$	$9 \cdot 10^{-4}$	$9 \cdot 10^{-4}$	$9 \cdot 10^{-4}$	$9 \cdot 10^{-4}$	$9 \cdot 10^{-4}$
R (−)	8.34	8.77	8.86	8.98	8.32	8.98	8.79	8.99
k (day^{-1})	8.11	7	8.79	7.86	7	7	11	11
F_1 (−)	0.5	0.5	0.5	0.5	0.5	0.5	0.5	0.5
F_2 (−)	0.1	0.1	0.1	0.1	0.1	0.1	0.1	0.1

Figure 13. Diagrams of C_{VAD} and C_{SAT} concentrations for flow paths 1 and 4 towards Jezerce well obtained with optimal combinations of the variation parameters values (Table 6).

5. Discussion and Conclusions

This paper presents a methodology for determining the die-off coefficient of faecal indicator bacteria, ENT, in terms of transport through the karst environment. The methodology assumes the successive application of statistical, numerical and analytical modelling in order to define the self-purification capacity of the analysed aquifer (the effects of sorption and die-off expressed by the corresponding coefficients).

With the transfer function, used as a method of time series analysis, a specific answer to the question of a dominant trigger of the enlarged ENT concentrations in the wells was obtained. In addition, time series analysis gave an insight into the average groundwater velocities later used to determine the potential source of pollution. In the applied analytical model, the calculation of ENT concentration removal was divided into two parts, the unsaturated and saturated transport phase. Removal of ENT concentrations in the unsaturated zone, due to the low percolation velocity and small size of the fractures, binds to two processes: natural die-off and sorption. By transporting through a saturated environment where much higher seepage velocities occur, the impact of sorption is negligible and the dominant process of ENT removal is a natural die-off.

The influence of the individual parameters used in the analytical model was analysed by sensitivity analysis. The diagram in Figure 11 shows the influence of the turbulent filtration coefficient value at variable ΔC. It is evident that ΔC is smaller in the case of a turbulent filtration coefficient of $K = 0.5$ m/s, which is also confirmed by the lower values of the statistical criterion RMSE. Also, the calculated average seepage velocity (Equation (9)) for the conductivity coefficient $K = 0.5$ m/s for the time period 1 January 2012—19 October 2016 is 1.26 cm/s and maximum 2.3 cm/s. Such values are consistent with the apparent velocity values in the area obtained from tracer tests [40]. Therefore, in further analysis, the value of the turbulent filtration coefficient $K = 0.5$ m/s was used. The sensitivity analysis for the variable v_{VAD} was conducted for the range of 10^{-4} to 10^{-2} m/s. From Figure 12 the exponential increase of the RMSE is clearly visible from the value $v_{VAD} = 10^{-3}$ m/s upwards. The difference of the statistical criterion RMSE between 10^{-3} m/s and 10^{-2} m/s is approximately seven orders of magnitude (RMSE $\approx 6.5 \cdot 10^7$ for $v_{VAD} = 10^{-2}$ m/s, RMSE ≈ 20 for $v_{VAD} = 10^{-3}$ m/s). The analysis showed that the percolation velocity of 10^{-4} m/s results in the complete removal of faecal indicator bacteria to the contact with the saturated zone due to the extremely slow percolation which leaves enough time for ENT removal. With such velocity values, ENT to the saturated zone can only break through if ignoring the sorption effect, i.e., if $k = 0$ (Equation (6)). On the other hand, due to

the velocity of 10^{-2} m/s, the percolation is rapid and ENT encounter the saturated zone in virtually unchanged concentration. Therefore, value of the percolation velocity of $v_{VAD} = 9 \cdot 10^{-4}$ m/s was adopted, which, according to [35], corresponds to the mean velocity in three recognised phases of percolation.

The mean value of the total die-off coefficient by transport through the unsaturated zone in the analysed case is $k_{tot} = 8.25$. Within the saturated zone the total die-off coefficient k_{tot} is within the limits of 0.1 and 0.5. From the results of the analysis it can be concluded that the unsaturated zone represents a suitable environment for ENT removal (reduction of six orders of magnitude in relation to the initial concentration) where sorption is the dominant process of natural ENT removal.

Further research is planned to focus on the unsaturated zone and the processes within it, especially from the aspect of removing pollution from water. The significance of the unsaturated zone in pollution removal from the water has been proved by the implementation of this methodology.

Author Contributions: Ž.Š. and G.L. collected in-situ and archive data consider analysed catchment and aquifer; M.G. performed the statistical simulations and analysed the data; Ž.Š. and G.L. designed the analytical model; Ž.Š. designed the numerical model, Ž.Š., G.L. and M.G. wrote the paper.

References

1. Mangin, A. Insights Into Hydrodynamic Behaviour of Karst Aquifers. Ph.D. Thesis, Université de Dijon, Dijon, France, 1975.
2. Drogue, C. Hydrodynamics of karstic aquifers: Experimental sites in the mediterranean karst, Southern France. *Int. Contrib. Hydrogeol.* **1992**, *13*, 133–149.
3. Doerfliger, N.; Jeannin, P.Y.; Zwahlen, F. Water vulnerability assessment in karst environments: a new method of defining protection areas using a multi-attribute approach and GIS tools (EPIK method). *Environ. Geol.* **1999**, *39*, 165–176, doi:10.1007/s002540050446. [CrossRef]
4. Lee, E.S.; Krothe, N.C. A four-component mixing model for water in a karst terrain in south-central Indiana, USA. Using solute concentration and stable isotopes as tracers. *Chem. Geol.* **2001**, *179*, 129–143, doi:10.1016/S0009-2541(01)00319-9. [CrossRef]
5. Perrin, J. A Conceptual Model of Flow and Transport in a Karst Aquifer Based on Spatial and Temporal Variations of Natural Tracers. Ph.D. Thesis, Université de Neuchâtel, Neuchâtel, Switzerland, 2003.
6. Teutsch, G.; Sauter, M. Distributed parameter modelling approaches in karst hydrological investigations. *Bull. Hydrogeol.* **1998**, *16*, 99–110.
7. Kuniansky, E.L.; Fahlquist, L.; Ardis, A.F. Travel Times Along Selected Flow Paths of the Edwards Aquifer, Central Texas. *USGS Water Resour. Invest. Rep.* **2001**, *1*, 69–77.
8. Scanlon, B.R.; Mace, R.E.; Barrett, M.E.; Smith, B. Can we simulate regional groundwater flow in a karst system using equivalent porous media models? Case study, Barton Springs Edwards aquifer, USA. *J. Hydrol.* **2003**, *276*, 137–158, doi:10.1016/S0022-1694(03)00064-7. [CrossRef]
9. Kuniansky, E.L.; Ardis, A.F. *Hydrogeology and Ground-Water Flow in the Edwards-Trinity Aquifer System, West-Central Texas U. S. Department of the Interior*; Technical Report; U.S. Geological Survey: Reston, VA, USA, 2004.
10. McGurk, B.; Presley, P.F. *Simulation of the Effects of Groundwater Withdrawals on the Floridan Aquifer System in East-Central Florida: Model Expansion and Revision*; Technical Report; St. Johns River Water Management District Technical Publication SJ2002-3: Platka, FL, USA, 2002.
11. Sepulveda, N. *Simulation of Ground-Water Flow in the Intermediate and Floridan Aquifer Systems in Peninsular Florida*; Technical Report; U.S. Geological Survey Water-Resources Investigations Report 02-4009; USGS: Reston, VA, USA, 2002.

12. Agyei, E.; Munch, D.; Burger, P. Application of optimisation modeling to water resource planning in East-Central Florida. *Tech. Publ.* **2005**, *SJ2005-2*, 82.

13. Davis, B.J.H.; Katz, B.G. *Hydrogeologic Investigation, Water Chemistry Analysis, and Model Delineation of Contributing Areas for City of Tallahassee Public-Supply Wells*; Technical Report; U.S. Geological Survey: Tallahassee, FL, USA, 2007.

14. Grubbs, J.W.; Crandall, C.A. *Exchanges of Water between the Upper Floridan Aquifer and the Lower Suwannee and Lower Santa Fe Rivers, Florida*; Technical Report; Geological Survey (USGS): Santa Fe Rivers, FL, USA, 2007. doi:10.3133/pp1656C.

15. Davis, J.H.; Katz, B.G.; Griffin, D.W. Nitrate-N Movement in Groundwater From the Land Application of Treated Municipal Wastewater and Other Sources in the Wakulla Springs Springshed, Leon and Wakulla Counties, Florida, 1966–2018. *U.S. Geol. Surv. Sci. Invest. Rep.* **2010**, *5099*, 90, doi:10.3133/sir20105099. [CrossRef]

16. Sepulveda, N.; Tiedeman, C.; O'Reilly, A.; Davis, J.; Burger, P. *Groundwater Flow and Water Budget in the Surficial and Floridan Aquifer Systems in East-Central Florida*; Technical Report, U.S. Geological Survey Scientific Investigations Report 2012-5161; USGS: Reston, VA, USA, 2012.

17. Miles, R.J.; Borchelt, G.; Casaletto, D. Treatment of drip dispersed effluent in imported soils. Innovation in Soil-Based Onsite Wastewater Treatment. In Proceedings of the Soil Science Society of America, Albuquerque, NM, USA, 7–8 April 2014.

18. Siegrist, R.L. Engineering of a Soil Treatment Unit as a Unit Operation in an Onsite Wastewater System. *Innov. Soil Based Onsite Wastewater Treat.* **2014**, *1*, 13–26, doi:10.13031/2013.23990. [CrossRef]

19. Morrissey, P.J.; Johnston, P.M.; Gill, L.W. The impact of on-site wastewater from high density cluster developments on groundwater quality. *J. Contam. Hydrol.* **2015**, *182*, 36–50, doi:10.1016/j.jconhyd.2015.07.008. [CrossRef]

20. Zyman, J.; Sorber, C.A. Influence of Simulated Rainfall on the Transport and Survival of Selected Indicator Organisms in Sludge-Amended Soils. *J. Water Poll. Control Fed.* **1988**, *60*, 2105–2110.

21. Guber, A.K.; Shelton, D.R.; Pachepsky, Y.A. Transport and Retention of Manure-Borne Coliforms in Soil. *Vad. Zone J.* **2005**, *4*, 828–837, doi:10.2136/vzj2004.0097. [CrossRef]

22. Cey, E.E.; Rudolph, D.L.; Passmore, J. Influence of macroporosity on preferential solute and colloid transport in unsaturated field soils. *J. Contam. Hydrol.* **2009**, *107*, 45–57, doi:10.1016/j.jconhyd.2009.03.004. [CrossRef]

23. Jiang, S.; Pang, L.; Buchan, G.D.; Šimůnek, J.; Noonan, M.J.; Close, M.E. Modeling water flow and bacterial transport in undisturbed lysimeters under irrigations of dairy shed effluent and water using HYDRUS-1D. *Water Res.* **2010**, *44*, 1050–1061, doi:10.1016/j.watres.2009.08.039. [CrossRef]

24. Liping, P.; Malcolm, M.; Jacqueline, A.J.Š.; Murray, C.; Hector, R. Modeling Transport of Microbes in Ten Undisturbed Soils under Effluent Irrigation. *Vad. Zone J.* **2008**, *7*, 97, doi:10.2136/vzj2007.0108. [CrossRef]

25. Wang, Y.; Bradford, S.A.; Šimůnek, J. Transport and fate of microorganisms in soils with preferential flow under different solution chemistry conditions. *Water Res. Res.* **2013**, *49*, 2424–2436, doi:10.1002/wrcr.20174. [CrossRef]

26. Firouzi, A.F.; Homaee, M.; Klumpp, E.; Kasteel, R.; Tappe, W. Bacteria transport and retention in intact calcareous soil columns under saturated flow conditions. *J. Hydrol. Hydromech.* **2015**, *63*, 102–109, doi:10.1515/johh-2015-0020. [CrossRef]

27. Foppen, J.W.A.; Schijven, J.F. Evaluation of data from the literature on the transport and survival of Escherichia coli and thermotolerant coliforms in aquifers under saturated conditions. *Water Res.* **2006**, *40*, 401–426, doi:10.1016/j.watres.2005.11.018. [CrossRef]

28. Rogers, S.W.; Donnelly, M.; Peed, L.; Kelty, C.A.; Mondal, S.; Zhong, Z.; Shanks, O.C. Decay of bacterial pathogens, fecal indicators, and real-time quantitative PCR genetic markers in manure-amended soils. *Appl. Environ. Microbiol.* **2011**, *77*, 4839–4848, doi:10.1128/AEM.02427-10. [CrossRef]

29. Alexandria, B.B.; Sassoubre, L.M. Enterococci as Indicators of Environmental Fecal Contamination. In *Enterococci: From Commensals to Leading Causes of Drug Resistant Infection*; Gilmore, M.S., Clewell, D.B., Ike, Y., Shankar, N., Eds.; Massachusetts Eye and Ear Infirmary: Boston, UK, 2014; pp. 101–123. doi:10.1016/j.jinteco.2006.12.001.

30. Oladeinde, A.; Bohrmann, T.; Wong, K.; Purucker, S.T.; Bradshaw, K.; Brown, R.; Snyder, B.; Molina, M. Decay of Fecal Indicator Bacterial Populations and Bovine-Associated Source-Tracking Markers in Freshly Deposited Cow Pats. *Appl. Environ. Microbiol.* **2014**, *80*, 110–118, doi:10.1128/AEM.02203-13. [CrossRef] [PubMed]

31. John, D.E.; Rose, J.B. Review of Factors Affecting Microbial Survival in Groundwater. *Environ. Sci. Technol.* **2005**, *39*, 7345–7356, doi:10.1021/es047995w. [CrossRef]

32. Althaus, H.; Jung, K.D.; Matthess, G.; Pekdeger, A. Lebensdauer von Bacterien und Viren in Grundwasserleitern. *Umweltbundesamt Mater.* **1982**, *1*, 190.

33. Artz, R.R.; Killham, K. Survival of Escherichia coli O157:H7 in private drinking water wells: Influences of protozoan grazing and elevated copper concentrations. *FEMS Microbiol. Lett.* **2002**, *216*, 117–122, doi:10.1016/S0378-1097(02)01002-9. [CrossRef] [PubMed]

34. Schwarz, K.; Barth, J.A.; Postigo-Rebollo, C.; Grathwohl, P. Mixing and transport of water in a karst catchment: A case study from precipitation via seepage to the spring. *Hydrol. Earth Syst. Sci.* **2009**, *13*, 285–292, doi:10.5194/hess-13-285-2009. [CrossRef]

35. Williams, P.W. The role of the epikarst in karst and cave hydrogeology: A review. *Int. J. Speleol.* **2008**, *37*, 1–10, doi:10.5038/1827-806X.37.1.1. [CrossRef]

36. Kuk, V.; Prelogović, E.; Dragičević, I. Seismotectonically Active Zones in the Dinarides. *Geol. Croat.* **2000**, *53*, 295–303.

37. Majcen, Ž.; Korolija, B. *Osnovna Geološka Karta SFRJ 1:100.000, List Zadar L33–139, (Basic Geological Map of the SFRY, scale 1:100.000, Zadar Sheet)*; Technical Report; Institut za geološka istraživanja Zagreb (1963–1969), Savezni Geološki Zavod: Beograd, Serbia, 1973.

38. Vlahović, I.; Tišljar, J.; Velić, I.; Matičec, D. Evolution of the Adriatic Carbonate Platform: Palaeogeography, main events and depositional dynamics. *Palaeogeogr. Palaeoclimatol. Palaeoecol.* **2005**, *220*, 333–360, doi:10.1016/j.palaeo.2005.01.011. [CrossRef]

39. Hrvatski Geološki Institut (HGI). *Hidrogeološki Elaborat Zona Sanitarne Zaštite Crpilišta Zadarskog Vodovoda (Zdenci B-4 i B-5, Jezerce, Oko, Boljkovac i Golubinka) u Sklopu Hidrogeološkog Sustava Bokanjac-Poličnik*; Technical Report; Hrvatski geološki institut (Croatian Geological Survey): Zagreb, Croatia, 2013.

40. Pavičić, A., Terzić, J. *Hidrogeološki i Geofizički Istraživački Radovi za Mikrozoniranje Poslovne Zone "Bokanjac" kod Zadra, (Hydrogeological and Geophysical Research for the Micro Zoning of the Bokanjac Business District Near Zadar)*; Technical Report, Fond HGI 14/2006; Hrvatski geološki institut (Croatian Geological Survey): Zagreb, Croatia, 2006.

41. Fritz, F. *Ravni Kotari–Bukovica, Hidrogeološka Studija (Ravni Kotari–Bukovica, Hydrogeological Study)*; Technical Report, Archive of the Croatian Geological Survey; Hrvatski geološki Institut (Croatian Geological Survey): Zagreb, Croatia, 1976.

42. Geotehnika. *Vodoistražni radovi Zadar, Knjiga III—Vodostaji*; Professional Project: Water research works in the wider area of Zadar; City Waterworks Zadar: Zadar, Croatia, 1968.

43. Young, P.C.; Tych, W.; Taylor, C.J. The Captain Toolbox for Matlab. *IFAC Proc. Vol.* **2009**, *42*, 758–763, doi:10.3182/20090706-3-FR-2004.00126. [CrossRef]

44. Young, P.C. *Recursive Estimation and Time-Series Analysis*, 2nd ed.; Springer: Berlin/Heidelberg, Germany, 2011; p. 504. doi:10.1007/978-3-642-21981-8.

45. Young, P.C.; Taylor, C.J. Recent Developments in the CAPTAIN Toolbox for Matlab. *IFAC Proc. Vol.* **2012**, *45*, 1838–1843, doi:10.3182/20120711-3-BE-2027.00096. [CrossRef]

46. Box, G.E.P.; Jenkins, G.M. *Time Series Analysis: Forecasting and Control*; Holden-Day series in time series analysis and digital processing, Holden-Day; John Wiley & Sons: Hoboken, NJ, USA, 1976.

47. Jourde, H.; Mazzilli, N.; Lecoq, N.; Arfib, B.; Bertin, D. KARSTMOD: A Generic Modular Reservoir Model Dedicated to Spring Discharge Modeling and Hydrodynamic Analysis in Karst. In *Hydrogeological and Environmental Investigations in Karst Systems*; Andreo, B., Carrasco, F., Durán, J.J., Jiménez, P., LaMoreaux, J.W., Eds.; Springer: Berlin/Heidelberg, Germany, 2015; pp. 339–344. doi:10.1007/978-3-642-17435-3_38.

48. Bonacci, O. Monthly and annual effective infiltration coefficients in Dinaric karst: Example of the Gradole karst spring catchment. *Hydrol. Sci. J.* **2010**, *46*, 287–299, doi:10.1080/02626660109492822. [CrossRef]

49. Lončar, G.; Šreng, Ž.; Bekić, D.; Kunštek, D. Hydraulic-Hydrology Analysis of the Turbulent Seepage Flow within Karst Aquifer of the Golubinka Spring Catchment. *Geofluids* **2018**, *2018*, 12, doi:10.1155/2018/6424702. [CrossRef]
50. Jović, V. *Analysis and Modelling of Non-Steady Flow in Pipe and Channel Networks*; Wiley: Split, Croatia, 2013; p. 544.
51. Bandy, A.M. Mobility of *Escherichia coli* within Karst Terrains, Kentucky, USA. Ph.D. Thesis, University of Kentucky, Lexington, KY, USA, 2016.